Research Article

Facile Preparation of Optically Tailored Hybrid Nanocomposite

Susana Fernández de Ávila,[1] J. C. Ferrer,[1] J. L. Alonso,[1] R. Mallavia,[2] and B. Rakkaa[1]

[1] *Departamento de Ingeniería de Comunicaciones, Universidad Miguel Hernández, Edificio Innova, Avda. de la Universidad s/n, Elche, 03202 Alicante, Spain*

[2] *Instituto de Biología Molecular y Celular, Universidad Miguel Hernández, Edificio Torregaitán, Avda. de la Universidad s/n, Elche, 03202 Alicante, Spain*

Correspondence should be addressed to Susana Fernández de Ávila; s.fdezavila@umh.es

Lead sulfide nanoparticles (PbS NPs) have been synthesized directly in poly[2-methoxy-5-($3'$,$7'$-dimethyloctyloxy)-1,4-phenylenevinylene] (MDMO-PPV) semiconducting polymer by a simple low temperature method. Hybrid solutions with different concentrations of PbS with respect to the polymer have been prepared and characterized first in solution and then as thin film nanocomposites deposited on quartz substrates by spin coating. Quenching of photoluminescence emission is observed both in solutions and thin films when the ratio of PbS NPs increases with respect to the polymer, suggesting the occurrence of Dexter energy transfer from the polymer to the PbS NPs. Optical absorption is markedly increased for hybrid solutions compared to pure polymer. In thin nanocomposite films an enhancement of absorbance is observed with increasing PbS NPs concentration, which is more pronounced below 400 nm. The reported results could lead to the development of a method for tailoring the optical response of devices based on PbS NP-polymer nanocomposite by controlling the PbS NP concentration inside the polymer matrix.

1. Introduction

Hybrid composites, based on inorganic semiconducting nanoparticles (NPs) embedded in organic or polymeric matrix, have been the subject of intensive research during the last decade [1–4].

These materials are particularly attractive if they can be easily synthesized and processed at low cost. Examples are nanocomposites processed from solution that can be cast by simple techniques, such as different printing technologies, drop-casting, or spin-coating, among others.

The use of such materials as active layers for several optoelectronic devices [5–8] is increasing the interest of studies on their optical properties.

In particular, nanocomposites of PbS NPs directly synthesized in a hosting polymer are interesting [9–12] due to the broad absorption band and large excitonic radius of PbS NPs which allows modulating the absorption edge from 3200 nm for the bulk, to 530 nm for very small nanocrystals [13].

Several methods can be used to synthesize PbS NPs. In contrast to hot injection routes such as the well-known TOP-TOPO method, we present here a very simple chemical colloidal method that can be carried out at low temperature, easing commercial scale production.

In this paper, we show that optical properties of a hybrid nanocomposite can be tailored by controlling its stoichiometric composition. In particular we prepare the composite by synthesizing PbS NPs directly in poly[2-methoxy-5-($3'$,$7'$-dimethyloctyloxy)-1,4-phenylenevinylene] (MDMO-PPV) semiconducting polymer as described in Section 2. Optical absorption and luminescence characterization are performed for solutions as well as spin-coated thin films with increasing PbS NPs to MDMO-PPV ratio. A decrease of photoluminescence (PL) intensity and an increase of optical absorption are found for higher PbS NPs concentrations in the composite. A remarkably strong and broad absorption is found for hybrid films which could be of interest for application in optoelectronic devices such as photodetectors or solar cells.

2. Materials and Methods

2.1. Synthesis of Hybrid Nanocomposite. The method employed for the synthesis of PbS NPs has been adapted from the approach developed by Dance et al. [14] to synthesize ZnS and CdS nanocrystals capped with thiophenol. Typically, to a solution of $Pb(NO_3)_2$ (1 mmol, 331.2 mg) in water (2 mL) and methanol (8 mL) at room temperature, a solution of 4-fluorothiophenol (6 mmol, 639 μL) in methanol (10 mL) was added. Reaction took place immediately, resulting in a yellow precipitate which was centrifuged and washed with methanol three times. The precipitate was vacuum dried obtaining a yellow powder which was soluble in dimethylsulfoxide (DMSO). Analysis of the powder by XPS suggests that its chemical composition is $Pb(SPhF)_2$ [15].

In a second step, MDMO-PPV and $Pb(SPhF)_2$ complex were dissolved in toluene and DMSO, respectively. Although MDMO-PPV cannot dissolve in DMSO, and $Pb(SPhF)_2$ cannot dissolve in toluene, both solutions were mixed and no precipitation or phase separation was observed using 4 : 1 toluene : DMSO ratio.

For the experiments presented in this paper, detailed stoichiometry is given in Section 4.

PbS nanoparticles are synthesized by adding a solution of sulfur in toluene to the polymer-complex solution. After several minutes orange solutions turned to brown dark indicating the formation of PbS NPs.

As it has been reported before [16] typical reaction of lead thiolates $[Pb(SR)_2$, R = organic group] with sulfur gives lead sulphide and the organic disulphide [RSSR] as reaction by-products. However, when this reaction takes place in a polymeric medium these organic by-products can be physically adsorbed on the surface of the inorganic sulfide [17], in our case the lead sulfide nanoparticle, producing polymer embedded cluster compounds like the nanocomposite presented in this work.

It is expected that this method allows the synthesis of nanoparticles minimizing the residues that would stay in the composite and could affect the performance of potential devices using this hybrid materials.

2.2. Thin Film Casting. Thin films were prepared by spin-coating on precleaned quartz substrates under ambient conditions.

Toluene based MDMO-PPV polymer film for reference was spin cast at 3000 rpm for two minutes. Solutions containing DMSO were spin cast at 500 rpm for two minutes and at 6000 rpm during one more minute. This last faster spin was intended to enhance dragging of residual DMSO solvent out of the samples surface. While toluene is quickly evaporated during spinning of the quartz substrate, the lower evaporation rate of DMSO avoids complete evaporation of this solvent from the sample at room temperature after the first spinning step, and small drops of DMSO can be seen on the surface of the films if the second spinning step is not applied.

Finally, annealing of all the samples at 90°C for 30 minutes was carried out to eliminate any solvent residue of thin films.

Thicknesses of the films obtained were in the range of 70–90 nm.

2.3. Structural Characterization. Transmission electron microscopy (TEM) measurements were done with a Jeol 2010 microscope operating at 200 keV. Samples for TEM were prepared by deposition of a single drop of the polymer-nanoparticles blend on a 300 mesh copper grid with a carbon film.

2.4. Optical Characterization. Optical absorbance spectra from solutions and thin films were acquired with a Shimazdu UV-1603 spectrometer. Photoluminescence measurements from solutions and thin films were performed with a Photon Technology International Quanta Master Model QM-62003SE spectrofluorometer.

3. Results and Discussion

For this study, two different batches of hybrid solutions were prepared.

The first batch of solutions was synthesized in order to study variations of optical properties just in solution (liquid state).

The second batch was prepared using higher concentrations for the purpose of casting thin films from each one of these solutions in order to evaluate the optical properties of the nanocomposite in the solid state, often preferred for optoelectronic devices fabrication.

3.1. Optical Characterization of Diluted Solutions. For this first experiment, two reference solutions were prepared. MDMO-PPV was dissolved in toluene (0.31 mg/mL) and $Pb(SPhF)_2$ complex was dissolved in DMSO (10 mg/mL). These two initial solutions are labeled as Solutions A and B, respectively. From them, five different new solutions were prepared as summarized in Table 1.

Solution C was obtained mixing solutions A and B in 4 : 1 volume ratio. Finally, four hybrid solutions were prepared by adding different volumes of a solution of sulfur in toluene 0.5%wt. The accurate composition of the solutions is outlined in Table 1.

Only absorption spectra of this batch are discussed here, but additional characterization can be found in [15].

Figure 1 shows absorbance spectra obtained for these solutions. Reference spectra of MDMO-PPV (solution A) and $Pb(SPhF)_2$ (solution B) are shown as thicker black solid line and thin dashed line, respectively. The typical absorption spectrum of MDMO-PPV with a maximum located around 495 nm is observed. The addition of $Pb(FPhS)_2$ complex to the polymer (solution C) is followed by an increasing absorption for wavelengths approximately below 410 nm. The yellow line in Figure 1 shows this result. As the sulfur solution is added to the polymer-precursor solution, the formation of nanocrystals proceeds and the absorption of the solution increases, extending the absorption band to the whole visible spectrum. Absorption corresponding to the sulfur solution is also shown by red symbols to exclude its contribution to the

TABLE 1: Details of solutions from first batch (used in Figures 1 and 2). Second column corresponds to volume ratios of MDMO-PPV in toluene and Pb(SPhF)$_2$ in DMSO reference solutions. Third column corresponds to the volume of sulfur, 0.5%wt in toluene, added to each solution to synthesize PbS NPs.

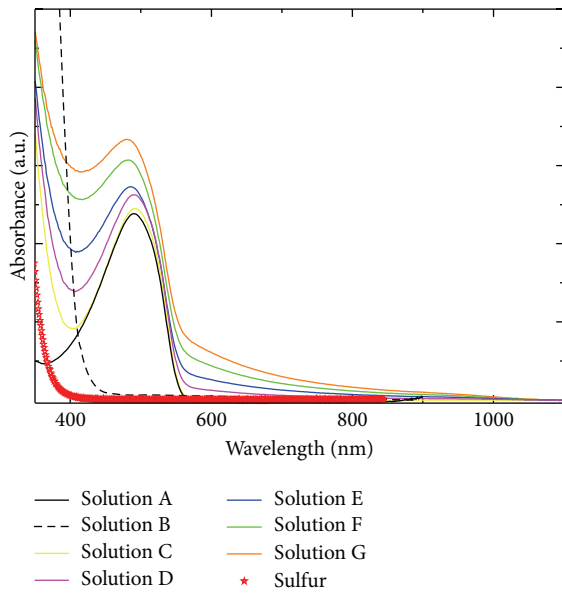| Solution label	MDMO-PPV : Pb(SPhF)$_2$ vol	S vol (μL)
A	1 : 0	0
B	0 : 1	0
C	4 : 1	0
D	4 : 1	25
E	4 : 1	50
F	4 : 1	75
G	4 : 1	100

FIGURE 1: UV-Vis-NIR absorption spectra for all the solutions shown in Table 1 (lines), and the sulfur solution (symbols) added to solutions D to G.

observed changes in absorbance spectra. For hybrid solutions D to G, the synthesis of PbS nanoparticles is responsible for absorption at longer wavelength region beyond 550 nm. Moreover, the increased absorption in the 350–450 nm range, compared to the pure polymer solution, is also due to PbS nanoparticles. This absorption rises as the volume of sulfur added increases because a higher ratio of NPs has been synthesized inside the MDMO-PPV solution.

TEM observations were performed to check the formation of PbS NPs in hybrid solutions. Figure 2 shows a high resolution image of an ensemble of NPs within the polymer matrix. This type of agglomeration has been previously reported in NPs hosted in polymers [18–20]. PbS crystals have an average diameter of 5 nm approximately and show good crystal quality. Image displayed in Figure 2(a) corresponds to solution G, the one with the highest volume of sulfur added. TEM measurements were also performed for the entire set of hybrid solutions presented in Table 1. Average

size of nanoparticles remains almost unchanged for all the analyzed solutions. The fact that the observed size is similar for samples with different PbS concentration (solutions D to G) suggests that the addition of further sulfur is followed by the formation of a higher number of NPs instead of increasing their size. Such a result has been previously found for similar nanoparticle-polymer composites [18].

The chemical composition of the nanoparticles synthesized by thiolate decomposition has been confirmed by measurements of the spacing of atomic planes from HRTEM images. The nanoparticle in Figure 2(b) shows the typical pattern of perpendicular atomic rows in a cubic structure observed along the ⟨100⟩ zone axis. The interplanar spacing measured from this image (0.297 nm) is in good agreement with the distance of {200} family planes of PbS. A similar study has been performed with the nanoparticle in Figure 2(c). The angle between the planes in the image matches the angle between the {111} family planes observed along the ⟨110⟩ zone axis. In this case, the atomic plane distance measured in the nanoparticle image (0.343 nm) coincides with the separation of {111} family planes of PbS as well.

Based on these results a second batch of solutions was prepared to evaluate the improvement of optical properties not only in solution, but also in thin solid films that might be used as photoactive layers for optoelectronic devices [6, 7, 20, 21].

3.2. Optical Characterization of Nanocomposite Thin Films. In this second experiment the solutions concentration was increased in order to obtain films with suitable thicknesses for optical characterization. The composition of each solution is detailed in Table 2.

Solution A$'$ was prepared dispersing 1 mg/mL MDMO-PPV in toluene, and for solution B$'$, 32 mg/mL Pb(SPhF)$_2$ was dissolved in DMSO. Solution C$'$ was obtained by mixing solutions A$'$ and B$'$ with a 4 : 1 volume ratio.

From previous experiments we had found that a portion of Pb(SPhF)$_2$ compound had not reacted to synthesize PbS NPs with the sulfur volumes used before. Thus, in this batch, the volume of sulfur solution added to solutions D$'$ to G$'$ was increased in order to reduce the excess of Pb(SPhF)$_2$ compound remaining in the nanocomposite.

To carry out the optical characterization of this new batch of solutions it was necessary to dilute them in order to avoid self-absorption. Quartz cells were filled with 100 μL of solution plus 2 mL of toluene to perform UV-Vis-NIR absorption spectroscopy and photoluminescence measurements of this second batch.

Optical absorbance spectra obtained from these solutions were very similar to those from previous experiment. Figure 3 shows the spectra corresponding to the MDMO-PPV reference solution (A$'$) and the four hybrid solutions (D$'$ to G$'$) normalized to the MDMO-PPV maximum absorption.

Again, for wavelengths longer than 550 nm the absorption increases from solution D$'$ to G$'$. This fact is due to the presence of PbS in the composite and it is an evidence of the formation of PbS NPs as the absorption edge is below
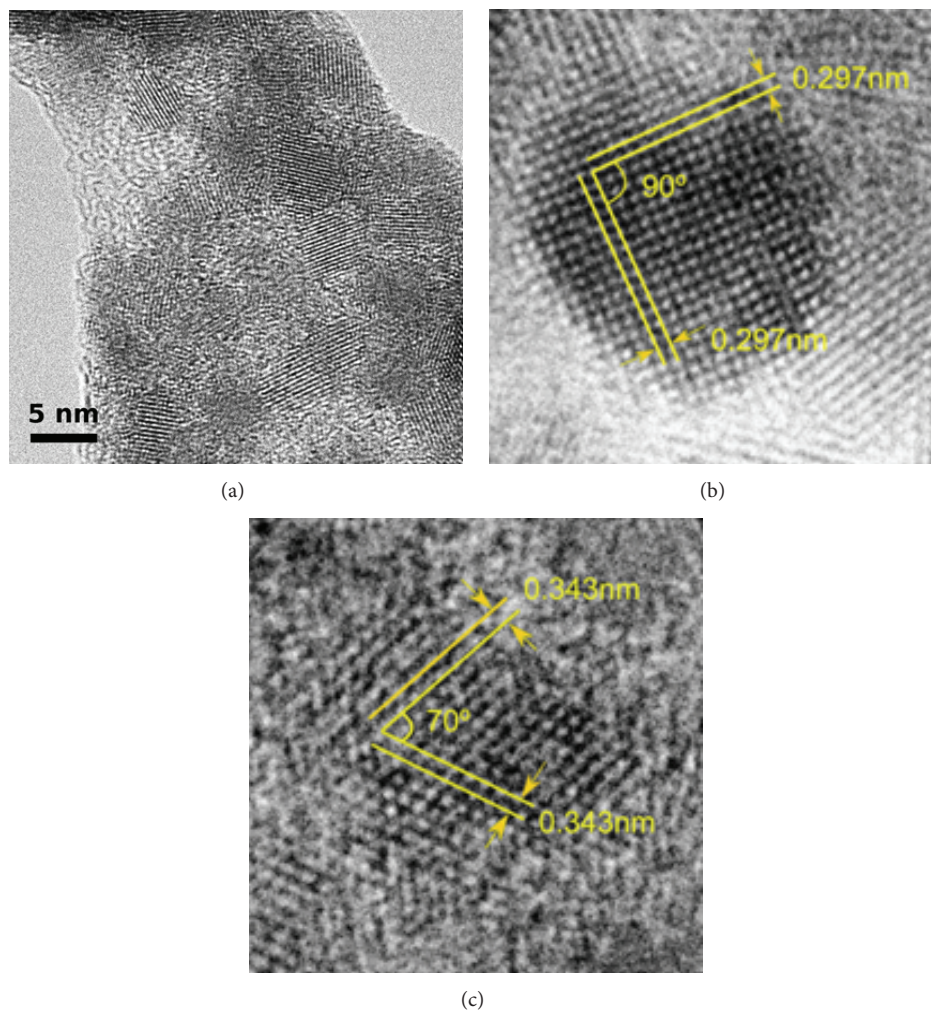
(a)

(b)

(c)

FIGURE 2: High resolution transmission electron microscopy images of PbS NPs embedded in MDMO-PV polymer matrix (solution G). (a) Average diameter of 5 nm can be clearly observed on several nanocrystals. Interplanar distances and angles measured on the PbS nanoparticles for (b) {200} and (c) {111} family planes.

TABLE 2: Details of solutions from second batch (used in Figures 3–6). Second column corresponds to volume ratios of MDMO-PPV in toluene and $Pb(SPhF)_2$ in DMSO reference solutions. Third column corresponds to the volume of sulfur, 0.5%wt in toluene, added to each solution to synthesize PbS NPs.

Solution label	MDMO-PPV : $Pb(SPhF)_2$ vol	S vol (μL)
A$'$	1 : 0	0
B$'$	0 : 1	0
C$'$	4 : 1	0
D$'$	4 : 1	200
E$'$	4 : 1	400
F$'$	4 : 1	800
G$'$	4 : 1	1600

1000 nm compared to 3200 nm expected for bulk material. Stronger absorption for these long wavelengths is related to the higher number of PbS NPs synthesized when the volume of sulfur increases.

A similar trend to that observed for diluted solutions is visible for the range of wavelengths below 450 nm. The dip observed around 410 nm for the hybrid solutions vanishes as the volume of sulphur increases. Only the spectrum corresponding to solution D$'$ seems to have weaker minimum than sample E$'$. A possible explanation for this behavior could be that this solution may still have a high portion of $Pb(SPhF)_2$ complex that did not react and it is enhancing the steeper slope of absorbance below 400 nm wavelength.

Additionally, it can be observed that the maximum of the absorbance spectra is slightly blue shifted for the hybrid solutions compared to the one of the MDMO-PPV polymer. This is a consequence of the competition between the reduction of the sharp absorption edge from solution B and the increasing contribution of the PbS NPs absorbance. This behavior was also observable in Figure 1.

Photoluminescence measurements of the solutions from Table 2 were also performed and their spectra are shown in Figure 4.
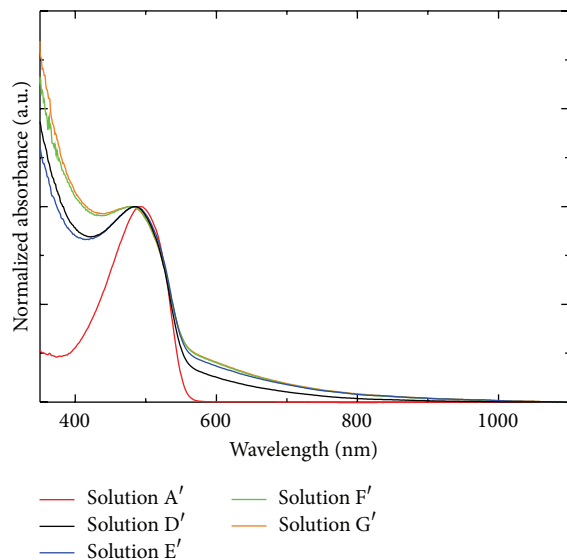
FIGURE 3: Normalized optical absorption of hybrid solutions from Table 2. The spectra are normalized with respect to the absorption maximum of the polymer reference solution A′ (shown as a red line).

Spectrum from the Pb(SPhF)$_2$ complex solution (B′) is shown with a black dashed line. An excitation wavelength of 300 nm was used for this measurement. The emission intensity was very low and blue shifted compared to the rest of solutions, confirming than emission observed for hybrid nanocomposite is only coming from the polymer and PbS nanoparticles in the solution.

An excitation wavelength of 450 nm was used for PL measurements of solutions and films containing MDMO-PPV. Spectra from solution A′ (pure polymer reference) and from hybrid solutions D′ to G′ are quite similar. A double peak with maxima located at 560 nm and 595 nm, as it is known [22] for MDMO-PPV polymer emission, is observed for all these solutions. A quenching of PL intensity happens when S volume increases as we had reported for more diluted solutions [15]. This behavior has been also observed previously in similar hybrid materials such as MEH-PPV and PbS NPs [23] and it is explained through Dexter energy transfer from the polymer to the NPs. This quenching process is also an indication of charge transfer between the polymer and the PbS NPs, highly desirable for optoelectronic applications. The exciton photogenerated in the polymer is dissociated and transfers the electron to the PbS NP while the hole remains in the polymer.

Thin film nanocomposites were prepared by spin-coating from solutions A′, D′, E′, F′, and G′ as described in the experimental Section 3.1. PL spectra of these films are shown in Figure 5. Spectra from thin films follow the trend of the solutions. The quenching of the luminescence increases with the concentration of PbS NPs. Slightly red-shifted and wider emission peaks are found for the films as compared to solution spectra. This behavior has been observed before and it is typical for film spectra [4], where London dispersion forces are stronger and energy transfer to the lowest excited state should be more efficient than in solutions.
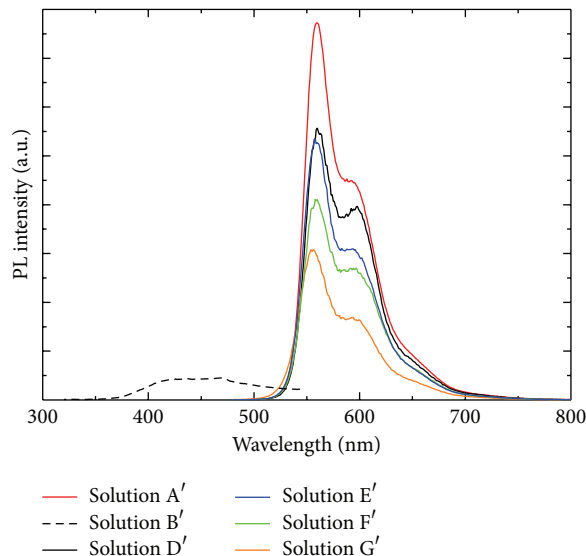

FIGURE 4: Photoluminescence spectra from solutions detailed in Table 2.
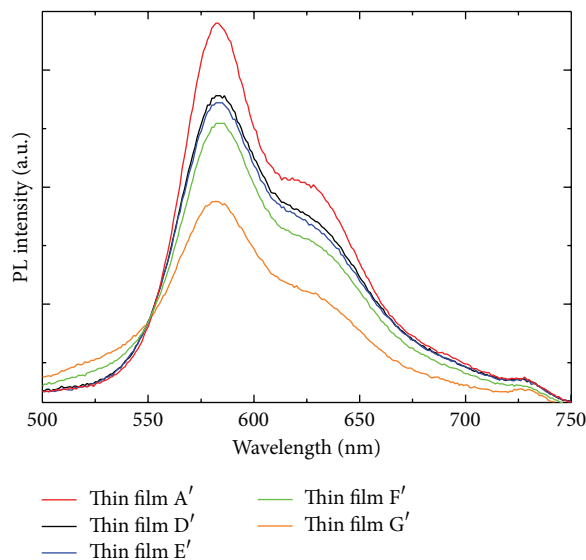

FIGURE 5: Photoluminescence spectra of thin films spin coated from solutions in Table 2.

Figure 6 shows the optical absorption spectra of the films cast from solutions in Table 2. The absorption peak, corresponding to the MDMO-PPV reference sample (A′), located around 494 nm, is visible in all hybrid nanocomposites just as a shoulder. An increased absorption is obtained for hybrid composites D′ to G′ when the portion of PbS NPs synthesized inside the polymer matrix increases. Contribution of PbS NPs can be seen not only for wavelengths higher than 550 nm but also towards UV range for wavelengths lower than 400 nm. These results are similar to those found for the solutions (Figures 1 and 3). However, it is noteworthy that composites with higher PbS NPs ratio show a continuously
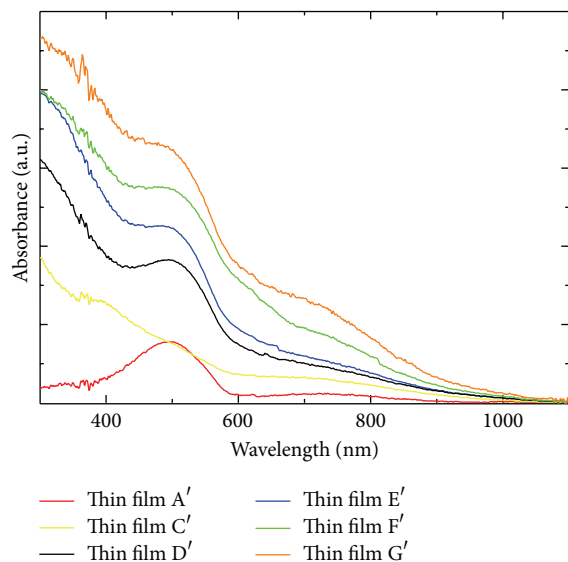
FIGURE 6: UV-Vis-NIR absorption of thin films spin coated from solutions in Table 2.

increasing absorption with decreasing wavelength, in contrast to solutions which still show wavelength ranges where absorption decreases with the reduction of wavelength. We guess that the route used for the direct synthesis of PbS NPs inside the polymer, with very few residues, plays a major role in the significant gain of absorbance observed in these nanocomposites.

This fact can be beneficial for the use of these films as photoactive materials. In particular, the enhanced absorption of hybrid polymer-PbS NPs nanocomposite compared to the pure polymer film indicates potential application of these composites as active layers for solar cells or photodetectors with improved absorbance while keeping flexibility, low cost, and light weight properties.

Further research is being performed in order to check electrical properties of these nanocomposite materials and evaluate the role of the reaction by-products acting as NP surfactants or as residues and their effect on potential optoelectronic applications.

4. Conclusions

We have demonstrated a simple, low-temperature full procedure to prepare hybrid nanocomposites by direct synthesis of PbS NPs inside MDMO-PPV polymer matrix. The ratio of PbS NPs synthesized can be changed through the volume of sulfur added, once the weight of $Pb(SPhF)_2$ compound in the solution is known. A partial quenching of the PL emission is observed in solution and thin films when PbS NPs are present in the MDMO-PPV polymer. This effect is attributed to Dexter energy transfer from the polymer to the NPs and it is desirable for potential optoelectronic applications of the composite.

In addition a higher optical absorption is measured for hybrid solutions compared to the pure polymer. This

enhancement is stronger for hybrid thin films where absorption spectra show a continuously decreasing slope from 300 nm through all the visible range. Application of these, suitable for high volume production, nanocomposites as active layers of photodetectors or photovoltaic devices is suggested.

Conflict of Interests

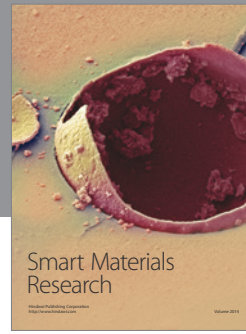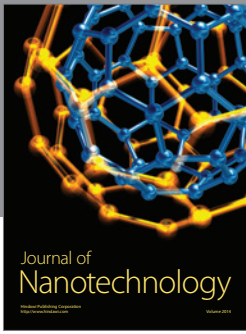The authors declare that there is no conflict of interests regarding the publication of this paper.

Acknowledgment

References

[1] T. Hanemann and D. V. Szabó, "Polymer-nanoparticle composites: from synthesis to modern applications," *Materials*, vol. 3, no. 6, pp. 3468–3517, 2010.

[2] A. C. Balazs, T. Emrick, and T. P. Russell, "Nanoparticle polymer composites: where two small worlds meet," *Science*, vol. 314, no. 5802, pp. 1107–1110, 2006.

[3] S. Kango, S. Kalia, A. Celli, J. Njuguna, Y. Habibi, and R. Kumar, "Surface modification of inorganic nanoparticles for development of organic-inorganic nanocomposites—a review," *Progress in Polymer Science*, vol. 38, no. 8, pp. 1232–1261, 2013.

[4] J. Li and J. Z. Zhang, "Optical properties and applications of hybrid semiconductor nanomaterials," *Coordination Chemistry Reviews*, vol. 253, no. 23-24, pp. 3015–3041, 2009.

[5] S. A. McDonald, P. W. Cyr, L. Levina, and E. H. Sargent, "Photoconductivity from PbS-nanocrystal/semiconducting polymer composites for solution-processible, quantum-size tunablein-frared photodetectors," *Applied Physics Letters*, vol. 85, no. 11, pp. 2089–2091, 2004.

[6] S. Günes, K. P. Fritz, H. Neugebauer, N. S. Sariciftci, S. Kumar, and G. D. Scholes, "Hybrid solar cells using PbS nanoparticles," *Solar Energy Materials & Solar Cells*, vol. 91, no. 5, pp. 420–423, 2007.

[7] A. Mansur, H. Mansur, and J. González, "Enzyme-polymers conjugated to quantum-dots for sensing applications," *Sensors*, vol. 11, no. 10, pp. 9951–9972, 2011.

[8] J. Chandrasekaran, D. Nithyaprakash, K. B. Ajjan, S. Maruthamuthu, D. Manoharan, and S. Kumar, "Hybrid solar cell based on blending of organic and inorganic materials—an overview," *Renewable and Sustainable Energy Reviews*, vol. 15, no. 2, pp. 1228–1238, 2011.

[9] J. N. Freitas, A. S. Gonçalves, and A. F. Nogueira, "A comprehensive review of the application of chalcogenide nanoparticles in polymer solar cells," *Nanoscale*, vol. 6, no. 12, pp. 6371–6397, 2014.

[10] R. Kostić, M. Romčević, N. Romčević et al., "Photoluminescence and far-infrared spectroscopy of PbS quantum dots—polyvinyl alcohol nanocomposite," *Optical Materials*, vol. 30, no. 7, pp. 1177–1182, 2008.

[11] B. R. Saunders and M. L. Turner, "Nanoparticle-polymer photovoltaic cells," *Advances in Colloid and Interface Science*, vol. 138, no. 1, pp. 1–23, 2008.

[12] A. Guchhait, A. K. Rath, and A. J. Pal, "To make polymer: quantum dot hybrid solar cells NIR-active by increasing diameter of PbSnanoparticles," *Solar Energy Materials & Solar Cells*, vol. 95, no. 2, pp. 651–656, 2011.

[13] Y. Wang, A. Suna, W. Mahler, and R. Kasowski, "PbS in polymers. From molecules to bulk solids," *The Journal of Chemical Physics*, vol. 87, no. 12, pp. 7315–7322, 1987.

[14] I. G. Dance, A. Choy, and M. L. Scudder, "Syntheses, properties, and molecular and crystal structures of (Me4N)4[E4M10(SPh)-16] (E = sulfur or selenium; M = zinc or cadmium): molecular supertetrahedral fragments of the cubic metal chalcogenide lattice," *Journal of the American Chemical Society*, vol. 106, no. 21, pp. 6285–6295, 1984.

[15] J. C. Ferrer, A. Salinas-Castillo, J. L. Alonso, S. F. de Ávila, and R. Mallavia, "Direct synthesis of PbS nanocrystals capped with 4-fluorothiophenol in semiconducting polymer," *Materials Chemistry and Physics*, vol. 122, no. 2-3, pp. 459–462, 2010.

[16] R. A. Shaw and M. Woods, "Preparation and some properties of lead thiolates," *Journal of the Chemical Society A: Inorganic, Physical, and Theoretical Chemistry*, pp. 1569–1571, 1971.

[17] L. F. Nicolais and G. Carotenuto, "Synthesis of polymer-embedded metal, semimetal, or sulfide clusters by thermolysis of mercaptide molecules dissolved in polymers," *Recent Patents on Materials Science*, vol. 1, pp. 1–11, 2008.

[18] J. C. Ferrer, A. Salinas-Castillo, J. L. Alonso, S. F. de Ávila, and R. Mallavia, "Synthesis and characterization of CdS nanocrystals stabilized in polyvinyl alcohol-sodium polyphosphate," *Materials Letters*, vol. 63, no. 6-7, pp. 638–640, 2009.

[19] M. Mukherjee, A. Datta, and D. Chakravorty, "Electrical resistivity of nanocrystalline PbS grown in a polymer matrix," *Applied Physics Letters*, vol. 64, no. 9, pp. 1159–1161, 1994.

[20] T. Rath and G. Trimmel, "In situ syntheses of semiconducting nanoparticles in conjugated polymer matrices and their application in photovoltaics," *Hybrid Materials*, vol. 1, pp. 15–36, 2013.

[21] D. Qi, M. Fischbein, M. Drndić, and S. Šelmić, "Efficient polymer-nanocrystal quantum-dot photodetectors," *Applied Physics Letters*, vol. 86, no. 9, Article ID 093103, pp. 1–3, 2005.

[22] J. P. Liu, S. C. Qu, X. B. Zeng et al., "Fabrication of ZnO and its enhancement of charge injection and transport in hybrid organic/inorganic light emitting devices," *Applied Surface Science*, vol. 253, no. 18, pp. 7506–7509, 2007.

[23] Y. Zhang and Z. Xu, "Direct observation of the size dependence of Dexter energy transfer from polymer to small PbS quantum dots," *Applied Physics Letters*, vol. 93, no. 8, Article ID 083106, 2008.